Electron Transfer to Photosystem 1 from Spinach Plastocyanin Mutated in the Small Acidic Patch: Ionic Strength Dependence of Kinetics and Comparison of Mechanistic Models†

Kenneth Olesen,‡ Mikael Ejdebäck,‡,§ Milan M. Crnogorac,|| Nenad M. Kostić,|| and Örjan Hansson*,‡

Biochemistry and Biophysics, Department of Chemistry, Göteborg University, P.O. Box 462, SE-405 30 Göteborg, Sweden, and Department of Chemistry, Iowa State University, Ames, Iowa 50011

Received June 1, 1999; Revised Manuscript Received October 11, 1999

ABSTRACT: A set of plastocyanin (Pc) mutants, probing the small acidic patch (Glu59, Glu60, and Asp61) and a nearby residue, Gln88, has been constructed to provide further insight into the electron transfer process between Pc and photosystem 1. The negatively charged residues were changed into their neutral counterparts or to a positive lysine. All mutant proteins exhibited electron transfer kinetics qualitatively similar to those of the wild type protein over a wide range of Pc concentrations. The kinetics were slightly faster for the Gln88Lys mutant, while they were significantly slower for the Glu59Lys mutant. The data were analyzed with two different models: one involving a conformational change of the Pc−photosystem 1 complex that precedes the electron transfer step (assumed to be irreversible) [Bottin, H., and Mathis, P. (1985) *Biochemistry 24*, 6453−6460] and another where no conformational change occurs, the electron transfer step is reversible, and dissociation of products is explicitly taken into account [Drepper, F., Hippler, M., Nitschke, W., and Haehnel, W. (1996) *Biochemistry 35*, 1282−1295]. Both models can account for the observed kinetics in the limits of low and high Pc concentrations. To discriminate between the models, the effects of added magnesium ions on the kinetics were investigated. At a high Pc concentration (0.7 mM), the ionic strength dependence was found to be consistent with the model involving a conformational change but not with the model where the electron transfer is reversible. One residue in the small acidic patch, Glu60, seems to be responsible for the major part of the ionic strength dependence of the kinetics.

Electron transfer (ET)[1] reactions play a central role in the metabolism of all living organisms, especially in energy-converting processes such as photosynthesis and respiration. These reactions have received considerable attention from both theoreticians and experimentalists; in particular, studies of photosynthetic reaction centers have provided much information (*1*, *2*). For these systems, the ET can be initiated with a flash and monitored through absorption changes with high time resolution. Another advantage with reaction centers is that the redox centers are located at fixed positions in an environment known from X-ray crystallographic studies. However, many biological ET reactions occur between soluble proteins, and the redox centers are not fixed in space. In addition to the elementary ET step that occurs in the reactive complex, there are now other processes that need to be understood: the diffusive approach of reactants (presumably guided by electrostatics), specific recognition between partners, possible rearrangement of the encounter complex to an active conformation, and dissociation of products (*2*).

One soluble redox protein in the photosynthetic ET chain is plastocyanin (Pc). It functions as an electron carrier between the membrane-bound protein complexes cytochrome (cyt) b_6f and photosystem 1 (PS1), and several of the non-ET steps listed above are involved in these reactions. The interaction with PS1 is particularly amenable to kinetic studies since the reaction can be initiated with a flash to photooxidize P700 (the reaction center chlorophyll of PS1) and the ET is readily monitored through absorption changes of the latter.

Pc is a rather small protein (10.4 kDa), and the redox center consists of a copper ion coordinated by amino acid residues in a special geometry, a so-called type 1 copper site. A charge transfer transition involving sulfur pπ orbitals of the Cys84 ligand and copper d orbitals gives the protein a strong blue color in the oxidized state. The structures of Pc isolated from a variety of organisms have been determined by X-ray crystallography and NMR, and recently, the crystal structure of a spinach Pc mutant was determined (*3*) (Figure 1). There are three regions that are important for the interaction with its redox partners, a hydrophobic patch and two acidic patches. The ET to PS1 is generally believed to occur through the solvent-exposed copper ligand His87 when the hydrophobic patch is in close contact with a shallow hydrophobic pocket on PS1 (*4*−*6*). The acidic patches are also involved in the binding. The negative charges are highly conserved among plants; however, a deletion of two negative residues in the small acidic patch is found in Pc sequences

† This work was supported by the Swedish Natural Science Research Council.

* Corresponding author. Fax: +46 31 773 3910. E-mail: Orjan.Hansson@bcbp.gu.se.

‡ Göteborg University.

§ Present address: Department of Natural Sciences, Skövde University, P.O. Box 408, SE-541 28 Skövde, Sweden.

|| Iowa State University.

[1] Abbreviations: cyt, cytochrome; ET, electron transfer; Pc, plastocyanin; PS1, photosystem 1.

10.1021/bi991242i CCC: $18.00
Published on Web 11/23/1999

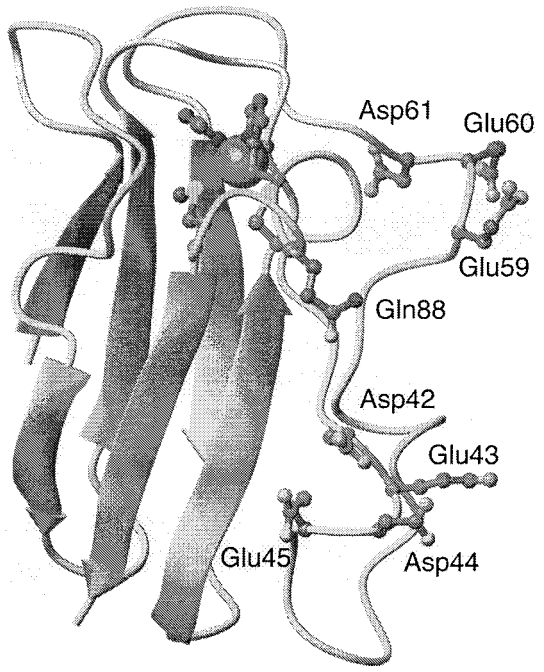

FIGURE 1: Schematic view of the structure of spinach plastocyanin. The amino acids in the large acidic patch (residues 42−45), small acidic patch (residues 59−61), and position 88 are labeled. Also shown as balls and sticks are the copper ligands. The hydrophobic patch is located above the copper ion in this orientation. The picture was drawn with MolMol (*34*) using coordinates from file 1ag6 (*3*) in the Brookhaven Protein Data Bank.

from parsley, barley, and algae. Other negative residues in the vicinity could compensate for this. The high degree of conservation of these patches and the ionic strength dependence of the reaction between Pc and cyt *f* or PS1 suggest an important function of these charges in the association of the reacting proteins and fine-tuning within the formed complex. The role of the acidic patches has therefore been studied extensively by cross-linking, chemical modification, competitive inhibition, and site-directed mutagenesis (*5*−*13*). A recent NMR study shows a close contact between the hydrophobic patch on Pc and the heme region on cyt *f* and also that electrostatic interactions between the two proteins are important (*14*). It has been suggested that electrostatic forces also take part in the interaction of Pc with the PsaF subunit of PS1 from higher plants, algae, and some cyanobacteria (*4*, *5*). This interaction probably first evolved for the reaction between PS1 and cyt c_6, but later also for the reaction with Pc (*15*).

The kinetic mechanism for the Pc to PS1 electron transfer reaction differs among organisms. In the cyanobacterium *Anabaena* sp. PCC 7119, no fast phase was detected in the P700 reduction kinetics and a simple collisional mechanism was proposed (*15*). For Pc and PS1 from green algae and higher plants, the reaction is more complicated as evidenced by the multiphasic kinetics. It has been suggested that a conformational change of the Pc−PS1 complex precedes the ET (*16*, *17*). An alternative model involves a reversible ET step in the reaction mechanism (*18*). Herein, we will refer to these models as the CC and RE models, respectively, and one aim of the present work is to identify the model which best describes the interaction. It will be shown that both models give rise to a similar set of differential equations but with different rate constants and initial conditions. The theoretical results are sufficiently general that they can be used for other systems of flash-induced ET between soluble redox partners where conformational changes or reversible ET might be involved.

In a recent paper, we presented results on the involvement of the large acidic patch (residues 42−45) in the reaction with PS1 (*11*). Strong effects were observed upon mutation of residues in positions 43 and 44 but weaker effects for a double mutant in the small acidic patch (residues 59−61); see Figure 1. Other studies have shown no (*10*) or only small impairment of the ET reaction upon mutation of residues in the small acidic patch (*5*, *19*). To clarify the role of this area, we have created single mutants where the original acidic amino acids have been replaced with their neutral counterparts or with the positive lysine. Another residue close to this area, Gln88, has also been replaced by a lysine. Altogether, seven mutant proteins have been produced, and their interactions with PS1 have been studied with flash photolysis over a large range of Pc concentrations (up to 1.0 mM). In addition, the dependence on ionic strength was studied at a high Pc concentration (0.7 mM) where the binding site on PS1 is saturated with Pc. Both kinetic models mentioned above can account for the Pc concentration dependence of the P700 reduction kinetics. However, the model involving a conformational change can better explain the ionic strength dependence.

MATERIALS AND METHODS

Site-Directed Mutagenesis, Expression, and Purification of Plastocyanin. Construction and production of the mutants were carried out as described by Ejdebäck et al. (*20*). Briefly, the mutants were constructed in a two-step PCR according to the method of Landt et al. (*21*). The plasmid pUG223t_r, which contains the wild type spinach gene, was used as a template, and the mutations were incorporated with mutagenic primers containing a mismatch. The PCR products were cloned into pUC18 and transformed into *Escherichia coli* DH5α cells. The gene for each mutant protein was sequenced and found to be correct.

The mutant proteins were overexpressed in the periplasm of *E. coli* RV308 grown at 37 °C and 150 rpm for 16 h. As an expression medium, LB broth containing 100 mg/L ampicillin, 100 μM $CuSO_4$, and 0.5 mM IPTG was used. Pc was extracted from the periplasm by osmotic lysis of the outer membrane followed by removal of some contaminating proteins by precipitation at pH 5.0. The protein was separated from other proteins by chromatography in an anion exchange step (Whatman DE32), in a size exclusion step (Sephacryl S-100HR), and on a Resource Q anion exchange FPLC column. To reduce the risk of loosening copper, all buffers except for the last dialysis buffer contained 100 μM $CuSO_4$.

Spectroscopic and Biochemical Characterization. All characterization experiments were performed as described previously (*6*, *11*). The p*I* of the mutant proteins was determined on a PhastGel Dry IEF rehydrated in Ampholine 3.5−5.0. Optical spectra were recorded between 240 and 900 nm on a Cary 4 UV/Vis spectrophotometer at room temperature. X-Band EPR spectra were recorded at 77 K with a Bruker ER 200D-SRC spectrometer. The reduction potentials were determined at pH 6, 7.5, and 9 by monitoring the absorbance at 597 nm as the ratio of potassium ferricyanide

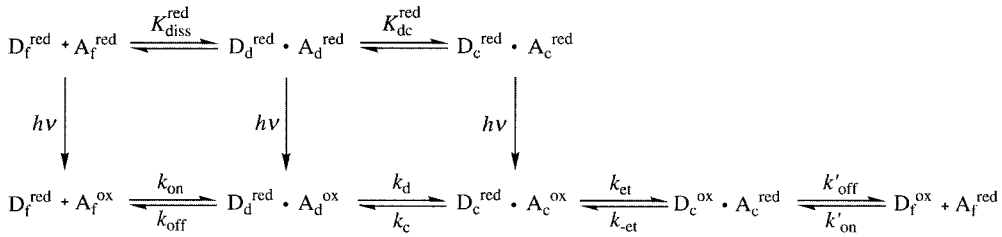

FIGURE 2: General kinetic model for the flash-induced electron transfer between a donor (D) and an acceptor (A). The complexation state of the reduced (red) and oxidized (ox) proteins is indicated with a subscript where the free proteins are denoted with an f and proteins bound in inactive (distant) or active (close) conformations are denoted with a d or c, respectively. The vertical arrows indicate the flash at time zero.

to ferrocyanide was varied. An average value from three independent measurements was determined.

Kinetic Measurements. The kinetics of the ET from Pc to PS1 were studied by monitoring the flash-induced absorption changes at 830 nm due to oxidized P700. Excitation of PS1 was obtained by a short flash from a Nd:YAG laser (Spectra Physics GCR 190-10, wavelength of 532 nm, pulse duration of 8 ns, pulse energy of 5 mJ/cm^2). The photooxidation and reduction of P700 were monitored with a continuous-wave diode laser (Melles Griot 06DLD203). A 1 mm × 10 mm × 45 mm (thickness × width × height) cuvette was placed with the flat surface at 90° to the excitation beam and at 45° to the measuring beam. In the studies of the ionic strength dependence, a 2 mm × 10 mm × 45 mm cuvette was used. All experiments were carried out at room temperature. PS1 with a chlorophyll *a*/*b* ratio of 6.6 was prepared in the dark using fresh, dark-adapted, hydroponically grown spinach according to the method of ref *22*. The standard reaction mixture contained, unless otherwise noted, Pc in 20 mM Tris buffer (pH 7.5), PS1 to a final chlorophyll concentration of 1 mg/mL, 2 mM sodium ascorbate, 0.1 mM methyl viologen, and 7 mM $MgCl_2$. This corresponds to an ionic strength of 40 mM, taking into account the contributions from the Tris buffer, the sodium ascorbate, and the $MgCl_2$. The sodium ascorbate was added to keep Pc reduced between the flashes. For a similar reason, methyl viologen was added to oxidize the F_A and F_B iron−sulfur centers in PS1. The absorption changes were monitored with a home-built detector consisting of an UDT PIN-10D silicon photodiode and different preamplifiers (bandwidth, 8 Hz to 14 or 30 MHz). For each Pc concentration, two sets of 16 traces with a spacing of 20 s were collected on two different time scales, averaged, and stored in digitized form using a Nicolet 490 oscilloscope. A sum of three decaying exponentials was fitted to the transients using the Levenberg−Marquardt algorithm in the Igor program (WaveMetrics Inc.).

Theory. A very general model for flash-induced ET between a diffusable donor D (Pc) and a photooxidizable acceptor A (P700) can be formulated as shown in Figure 2. Both D and A are reduced before the flash, and an equilibrium is set up between free molecules (subscript f) and complexes, which possibly can exist in different conformations, inactive ("distant", subscript d) and active ("close", subscript c). The overall effective dissociation constant is given by

$$(K_{diss}^{red})^{eff} = \frac{K_{diss}^{red}}{1 + K_{dc}^{red}}$$

where K_{diss}^{red} is the dissociation constant for the inactive conformation(s) and K_{dc}^{red} is an equilibrium constant for the conformational change. The superscript red signifies that A is reduced.

A flash at time zero oxidizes A (a suitable oxidant is presumed to accept the electron), and the equilibrium constants may now be different from those before the flash:

$$K_{diss} = \frac{k_{off}}{k_{on}} = rK_{diss}^{red}, \quad K_{dc} = \frac{k_d}{k_c} = qK_{dc}^{red}$$

where k_{off}, k_d, and k_c are first-order rate constants and k_{on} is a second-order rate constant. The effective dissociation constant when A is oxidized is given by the equation $K_{diss}^{eff} = K_{diss}/(1 + K_{dc})$. In the general case, the ET is reversible (rate constants k_{et} and k_{-et}) and the dissociation constant after the ET ($K'_{diss} = k'_{off}/k'_{on}$) is different from before the ET. The oxidized donor is subsequently restored to its reduced state by a suitable reductant.

Two of the commonly used models for the Pc−PS1 reaction can be viewed as special cases of the general model. In the model involving a conformational change (here denoted the CC model) introduced by Bottin and Mathis (*16*), the ET is irreversible ($k_{-et} = 0$) and the dissociation of products need not be considered. A similar model has earlier been suggested for the oxidation of soluble cyt *c* by reaction centers in purple bacteria (*23*); see, however, ref *24*. The CC model can account for the presence of two kinetic phases in the P700 reduction kinetics, even at saturating Pc concentrations, and the fact that the slow phase has a limiting rate constant of 10−20 × 10^3 s^{-1} (*6*). Recently, Drepper et al. (*18*) suggested an alternative model (here denoted the RE model) in which the conformational change is omitted (binding of Pc occurs directly to the active conformation), the ET is allowed to be reversible, and the dissociation of products is explicitly taken into account.

The CC and RE models can both be depicted with the reaction shown in Scheme 1. The C_i states and the rate

Scheme 1

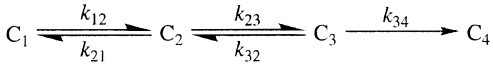

constants k_{ij} have different meanings in the two models as summarized in Table 1. The rate constant for binding of oxidized donor ($k_{43} = k'_{on}[D_f^{ox}]$) has been set equal to zero in the RE model. This is because $[D_f^{ox}]$ is low (less than or equal to the PS1 concentration) and also because oxidized

Table 1: Definitions of Quantities Used in the Two Models for the Reaction between Plastocyanin (D) and P700 (A) in Photosystem 1[a]

quantity	RE model	CC model
$c_1(t)$	$[A_f^{ox}]/A_{tot}$	$[A_f^{ox}]/A_{tot}$
$c_2(t)$	$[A_c^{ox}]/A_{tot}$	$[A_d^{ox}]/A_{tot}$
$c_3(t)$	$[A_c^{red}]/A_{tot}$	$[A_c^{ox}]/A_{tot}$
$c_4(t)$	$[A_f^{red}]/A_{tot}$	$[A_c^{red}]/A_{tot}$
$S(t)$	$c_1 + c_2$	$c_1 + c_2 + c_3$
k_{12}	$k_{on}[D_f^{red}]$	$k_{on}[D_f^{red}]$
k_{21}	k_{off}	k_{off}
k_{23}	k_{et}	k_d
k_{32}	k_{-et}	k_c
k_{34}	k'_{off}	k_{et}
c_{10}	$k_{21}/(k_{21} + rk_{12})$	$k_{21}qk_{32}/\pi^b$
c_{20}	$1 - c_{10}$	$rk_{12}qk_{32}/\pi^b$
c_{30}	0	$rk_{12}k_{23}/\pi^b$
c_{40}	0	0

[a] The RE model incorporates a reversible electron transfer step, and the CC model involves a conformational change between inactive and active conformations of the Pc−PS1 complex. The time-dependent normalized concentrations of the different C_i states are denoted by c_i ($i = 1$, 2, 3, or 4). A_{tot} is the total PS1 concentration, and S is the observed signal. The mechanistic rate constant for conversion from state C_i to C_j is designated with k_{ij}, and the initial concentrations are given by $c_{i0} = c_i(t = 0)$. See the legend of Figure 2 for the definitions of the other symbols. [b] $\pi = rk_{12}qk_{32} + k_{21}qk_{32} + rk_{12}k_{23}$.

Pc only binds weakly to PS1 (*18*). Replacing the Cu ion in Pc with Cd^{2+} (*25*) or Zn^{2+} (K. Olesen, unpublished results) to mimic the Cu^{2+} form also results in weak binding (if any).

The observed absorption signal $S(t)$ (due to oxidized P700, A^{ox}) and the initial conditions are different in the two models (Table 1), but their time evolution is governed by the same set of differential equations:

$$\dot{c}(t) = \mathbf{K}\cdot c(t), \quad c(0) = c_0$$

where $c(t)$ is a column vector of normalized concentrations $c_i(t)$ ($i = 1$, 2, or 3) and $\mathbf{K}$ is the matrix

$$\mathbf{K} = \begin{pmatrix} -k_{12} & k_{21} & 0 \\ k_{12} & -k_{21} - k_{23} & k_{32} \\ 0 & k_{23} & -k_{32} - k_{34} \end{pmatrix}$$

It is assumed that D is in sufficient excess over A so that the variation of $k_{12} = k_{on}[D_f^{red}]$ over time can be neglected. $\mathbf{K}$ will then be independent of time, and a solution of the differential equations can be written

$$c(t) = \mathbf{T}\cdot\mathbf{D}(t)\cdot\mathbf{T}^{-1}c_0$$

where $\mathbf{D}$ is a diagonal matrix with elements $d_i = \exp(-k_i t)$ ($i = 1$, 2, or 3 and $-k_i$ are eigenvalues of $\mathbf{K}$) and $\mathbf{T}$ contains the corresponding eigenvectors. Each component of $c(t)$ will consist of a sum of three exponentials, and the same is true for the observed signal:

$$S(t) = a_{vf}e^{-k_{vf}t} + a_f e^{-k_f t} + a_s e^{-k_s t}$$

The observed rate constants (subscripts vf, f, and s indicate very fast, fast, and slow components, respectively) depend only on the mechanistic rate constants through the eigenvalues of $\mathbf{K}$ but will vary with the donor concentration (due to the variation in k_{12}). On the other hand, the observed relative amplitudes (a_{vf}, a_f, and a_s) depend on both $\mathbf{K}$ and the initial conditions. The latter conditions are determined by the equilibrium set up before the flash, i.e., with A reduced (Table 1).

We have calculated the rate constants and amplitudes of the three exponentials in $S(t)$ as a function of donor concentration with the help of matrix diagonalization routines in MatLab (Math Works); see Figure 3 for an example. From simulations with a large range of plausible parameters, the following qualitative behavior is observed for both the CC and RE models. At very low donor concentrations, there are only two exponentials ($a_f \approx 0$). k_{vf} is approximately constant, while a_{vf} and k_s increase linearly with concentration. At intermediate concentrations of the donor (around 100 μM), all three amplitudes are non-zero, and thus, the observed signal is expected to consist of three exponentials. Finally, at high donor concentrations, there are again only two exponentials ($a_{vf} \approx 0$), and both the rate constants and the amplitudes of these are independent of the concentration ("saturation"). The value of k_f is similar to k_{vf} at very low donor concentrations.

The fact that the signal consists of only two exponentials in the limits of low and high donor concentrations suggests that the systems behavior can be approximated by simplified models. In the limit of low donor concentrations (when almost no donor is bound), we have done this by setting k_{32} (k_{-et} and k_c in the RE and CC models, respectively) equal to zero. In the other limit, we have neglected the C_1 state, i.e., assuming that the binding site on PS1 is saturated with Pc.

The resulting set of differential equations in each limit consists of only two coupled equations. Thus, standard methods can be used to derive analytical expressions for the amplitudes and rate constants of the two exponentials in the observed signal. The resulting equations are summarized in Table 2. Using these relations, it is possible to determine the mechanistic parameters from the observed parameters. As an example, expressions for k_{et} are given in the last row of Table 2 (the expression for the CC model has been derived under the assumption that $q = 1$). Specifically, the observed parameters at high donor concentrations (k_f, k_s, and a_f) can be used to calculate the equilibrium constants for the conformational change in the CC model ($K_{dc} = k_d/k_c$) and for the ET step in the RE model ($K_{et} = k_{et}/k_{-et}$). It turns out that the mathematical expressions are the same; i.e., $K_{dc} = K_{et}$.

In previous work, we have used approximate expressions to calculate k_d, k_c, and k_{et} from k_f, k_s, and a_f (denoted k_1, k_{2max}, and R_{max}, respectively, in the earlier work) (*17*). The approximate expressions result in k_c values that are 1.5 times larger than those calculated with the more correct relations derived in the work presented here.

RESULTS

Expression Yields

The expression yields of the mutants in the small acidic patch were similar to that of the wild type or slightly lower. A more drastic effect had the mutation Glu88Lys, which reduced the expression level 4-fold.

Spectroscopic and Biochemical Characterization

The isoelectric points of all mutants were higher than the wild type value (Table 3). This is expected since all mutations reduced the total negative charge of the proteins. A larger

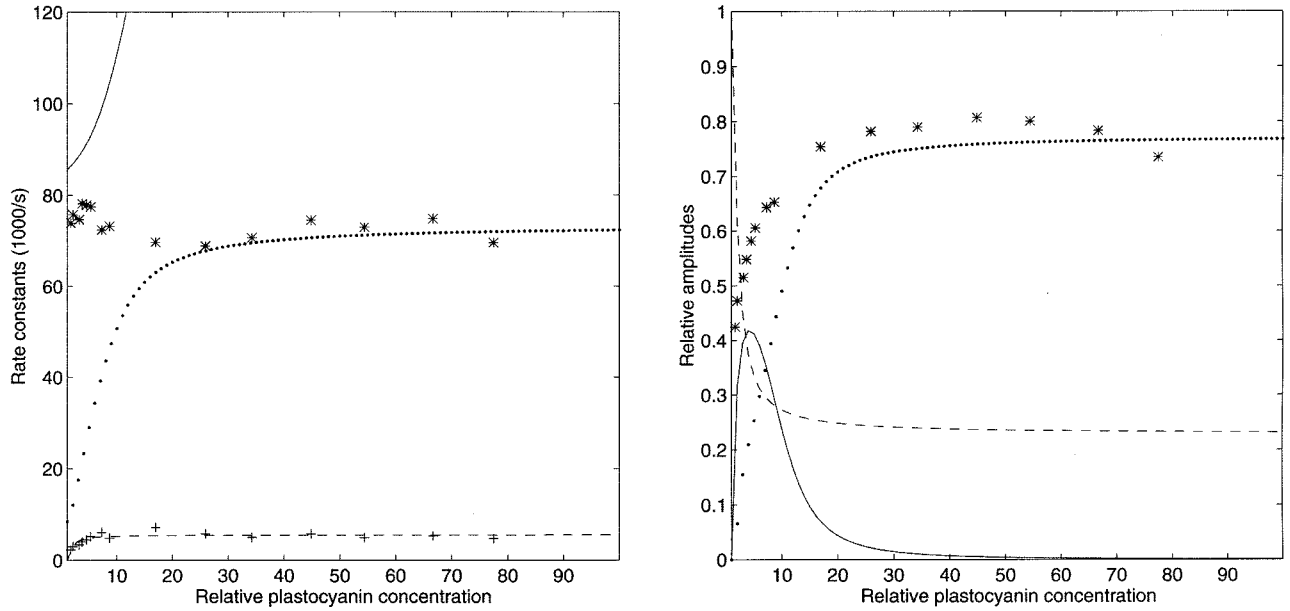

FIGURE 3: Kinetics of P700 reduction by the Asp61Lys plastocyanin mutant simulated assuming a model where the electron transfer is reversible (RE model). The rate constants (left) and relative amplitudes (right) of the three phases (—, very fast; •••, fast; and - - -, slow) in the decay of the normalized concentration of P700 were calculated as a function of plastocyanin concentration (a value of 100 on the abscissa corresponds to 1 mM) with matrix diagonalization methods (see the text for details). The mechanistic parameters were taken from Table 5 for the Asp61Lys mutant. The experimental values (* and +) are those obtained for this mutant.

Table 2: Expressions for the Observed Rate Constants (k_i) and Relative Amplitudes (a_i) in the Limits of Low and High Donor Concentrations As Derived from the Two Models for the Reaction between Plastocyanin and P700

quantity	RE model	CC model
	Low Donor Concentrations[a]	
k_{vf}	$k_{off} + k_{et}$	k_{et}
k_f	k'_{off}	$k_{off} + k_d$
k_s	$k_{et}k_{on}[D_f^{red}]/(k_{off} + k_{et})$	$k_dk_{on}[D_f^{red}]/(k_{off} + k_d)$
a_{vf}	$[k_{et}/(k_{off} + k_{et})]\{[D_f^{red}]/([D_f^{red}] + k_{diss}^{red})\}$	$k_dk_{on}[D_f^{red}]/[(k_{et} - k_{off} - k_d)k_{et}]$
a_f	0	0
	High Donor Concentrations	
k_{vf}	∞	∞
$k_f + k_s$	$k_{et} + k_{-et} + k'_{off}$	$k_c + k_d + k_{et}$
k_fk_s	$k_{et}\,k'_{off}$	k_dk_{et}
a_{vf}	0	0
a_f	$(k_{et} - k_s)/(k_f - k_s)$	$[1/(k_f - k_s)][k_fk_s/(qk_c + k_d) - k_s]$
k_{et}	$a_f(k_f - k_s) + k_s$	$(k_f + k_s) - \{k_fk_s/[a_f(k_f - k_s) + k_s]\}$

[a] The expressions for the CC model at low donor concentrations were derived under the assumption that $r = q = 1$ and $c_{10} = 1$.

Table 3: Isoelectric Points (p*I*), Reduction Potentials ($E°$), and Observed Kinetic Parameters Describing the Electron Transfer to Photosystem 1 at pH 7.5 for Wild Type and Mutant Plastocyanin[a]

plastocyanin	p*I*	$E°_{pH7.5}$ (mV)	k_f ($\times 10^3$ s^{-1})	k_{smax} ($\times 10^3$ s^{-1})	C_{ks} (μM)	a_{fmax}	C_{af} (μM)
wild type	3.82	384	80	12	43	0.67	26
Gln88Lys	4.03	379	87	14	42	0.79	26
Glu59Gln	3.90	388	71	10	29	0.67	40
Glu59Lys	4.08	394	67	10	53	0.56	38
Glu60Gln	3.90	384	77	6	13	0.59	4.7
Glu60Lys	4.15	388	69	4.8	6.4	0.73	3.5
Asp61Asn	3.95	390	80	11	38	0.70	26
Asp61Lys	4.09	393	73	5.7	8.8	0.77	8.3
Glu59Lys/Glu60Gln[b]	4.08	401	67	9.1	66	0.60	20

[a] The kinetic parameters were obtained from flash-induced absorbance changes of P700 as described in the text. [b] Data for this mutant were taken from ref *11*.

increase in the isoelectric point was observed for the lysine mutants of the small acidic patch, which can be explained by the reduction of the negative charge by 2 units. The integrity of the copper site was unchanged by the mutations as indicated by their wild type-like UV−vis and EPR spectra (*26*). The reduction potential exhibited no significant pH dependence in the investigated interval from pH 6.0 to 9.0, and the values at pH 7.5 are listed in Table 3.

Kinetic Measurements

The reactivity of the mutants toward PS1 was investigated with time-resolved absorption measurements at 830 nm. The

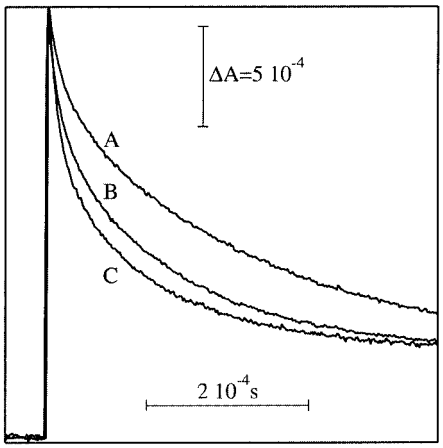

FIGURE 4: Absorption transients at 830 nm of photooxidized P700 in the presence of reduced wild type plastocyanin (B) or the mutants Glu59Lys (A) or Gln88Lys (C) at pH 7.5. Each sample contained photosystem 1 particles (chlorophyll concentration of 1 mg/mL) and 50 μM plastocyanin in a 20 mM Tris buffer supplemented with 0.1 mM methyl viologen, 2 mM sodium ascorbate, and $MgCl_2$ which was added to give a final total ionic strength of 40 mM in a cuvette with a 1 mm thickness. Each trace is the average of 16 flash-induced transients recorded with a spacing of 20 s. For clarity, only a fraction of the total recorded time scale is shown.

absorption coefficients of $P700^{ox}$ and Pc^{ox} are 5500 and 1000 M^{-1} cm^{-1}, respectively, while the reduced forms do not absorb at this wavelength (*17*, and references therein). As exemplified in Figure 4, flash illumination of a mixture of Pc^{red} and PS1 results in a rapid absorption increase, due to photooxidation of $P700^{red}$, which is followed by a decay that reflects the ET from Pc^{red}. When all $P700^{ox}$ has been reduced, there remains an absorption from Pc^{ox} that amounts to 18% (=1000/5500) of the initial amplitude, and subsequently, this absorption decays due to the reduction of Pc^{ox} by ascorbate on a time scale of seconds (*6*).

The reduction kinetics of $P700^{ox}$ are biphasic for all the mutants and for wild type Pc at the concentrations used to produce the data depicted in Figure 4, although there are differences in the details. The Glu59Lys mutant (Figure 4A) exhibits significantly slower kinetics than the wild type (Figure 4B), with less contribution from the fast phase and with a smaller rate constant for the slow phase. The Gln88Lys mutant is faster than the wild type in that the rate constants of both phases are higher (Figure 4C).

Effect of Pc Concentration on the Kinetics. The kinetics were examined at different Pc concentrations, up to 1.0 mM, and the absorption transients have been subjected to a curve-fitting analysis. The rate constant of the fast phase, k_f, was found to be independent of Pc concentration (Figure 5A), and the values obtained for the different mutants are summarized in Table 3. The rate constant of the slow phase, k_s (Figure 5B), as well as the fraction of the fast phase in the reduction kinetics of $P700^{ox}$, a_f (Figure 5C), display a saturation at high Pc concentrations. The limiting values, denoted k_{smax} and a_{fmax}, were obtained by fitting the data to rectangular hyperbolae (lines in panels B and C of Figure 5), and these values are listed in Table 3 together with the Pc concentrations C_{ks} and C_{af} at which half of the saturating values are obtained. As a comparison, we have also listed the parameters previously observed for the double mutant Glu59Lys/Glu60Gln (*11*).

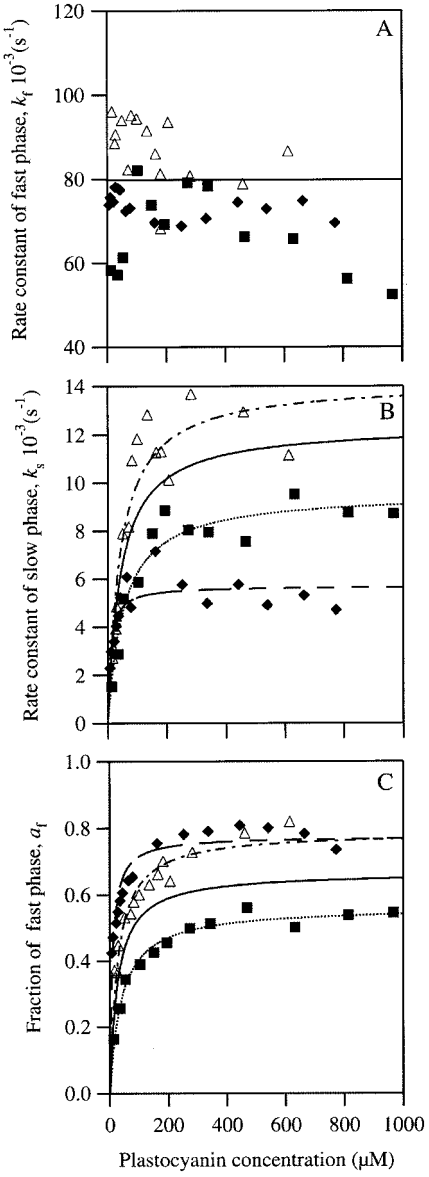

FIGURE 5: Effect of plastocyanin concentration on the reduction kinetics of photooxidized P700 by the plastocyanin mutants Glu59Lys (■), Asp61Lys (◆), and Gln88Lys (△). The experimental conditions were as described in the legend of Figure 4. The panels show the rate constants of the fast (k_f, A) and slow phases (k_s, B) and the fraction of the fast phase (a_f, C) as obtained from a curve-fitting analysis of absorption transients at 830 nm as described in the text. The curves in panels B and C are hyperbolic functions (parameters are given in Table 3) that best fit the k_s and a_f points, respectively. The solid lines represent averages of a large set of data for wild type plastocyanin.

The observed parameters are interpreted differently in the two mechanistic models as described in the Theory section in Materials and Methods. For the CC model, k_d, k_c, and k_{et} were calculated from the observed parameters in the limit of high Pc concentrations (k_f, k_{smax}, and a_{fmax}) given in Table 3 using the relations in Table 2. The results are listed in Table 4. The calculated k_d was then used together with the observed rate constant of the fast phase at low Pc concentrations and the slopes ($k'_s = k_{smax}/C_s$ and $a'_f = a_{fmax}/C_{af}$) to calculate k_{on} and k_{off}. The equilibrium constants K_{diss}, K_{dc}, and K_{diss}^{eff} were calculated as described in the Theory section in Materials and Methods.

Table 4: Calculated Mechanistic Parameters for Wild Type Plastocyanin and Mutants Describing the Electron Transfer to Photosystem 1 Assuming a Model That Involves a Conformational Change[a]

plastocyanin	k_{on} ($\times 10^9$ M^{-1} s^{-1})	k_{off} ($\times 10^3$ s^{-1})	K_{diss} (μM)	k_d ($\times 10^3$ s^{-1})	k_c ($\times 10^3$ s^{-1})	K_{dc}	K_{diss}^{eff} (μM)	k_{et} ($\times 10^3$ s^{-1})
wild type	1.5	57	37	13	4.1	3.2	8.7	75
Gln88Lys	1.8	63	35	15	2.6	5.7	5.2	84
Glu59Gln	1.8	45	25	11	3.4	3.1	6.0	67
Glu59Lys	1.0	46	47	10	4.9	2.2	15	61
Glu60Gln	5.2	67	13	6.4	3.4	1.9	4.4	73
Glu60Lys	10	60	6.0	4.9	1.5	3.2	1.4	67
Asp61Asn	1.7	59	34	12	3.4	3.5	7.5	76
Asp61Lys	7.4	61	8.2	5.8	1.4	4.2	1.6	71
Glu59Lys/Glu60Gln	0.9	52	60	9.8	4.1	2.4	18	62

[a] The parameters were calculated from the data in Table 3 as described in the text.

Table 5: Calculated Mechanistic Parameters for Wild Type Plastocyanin and Mutants Describing the Electron Transfer to Photosystem 1 Assuming a Model That Involves a Reversible Electron Transfer[a]

plastocyanin	k_{on} ($\times 10^9$ M^{-1} s^{-1})	k_{off} ($\times 10^3$ s^{-1})	K_{diss} (μM)	K_{diss}^{red} (μM)	k_{et} ($\times 10^3$ s^{-1})	k_{-et} ($\times 10^3$ s^{-1})	ΔE_c° (mV)	k'_{off} ($\times 10^3$ s^{-1})	K'_{diss} (mM)
wild type	0.40	23	56	28	57	18	30	17	1.1
Gln88Lys	0.41	16	38	27	72	12	45	17	0.54
Glu59Gln	0.48	20	42	43	51	16	29	14	0.56
Glu59Lys	0.29	25	87	43	42	19	20	15	2.1
Glu60Gln	0.73	29	40	5.0	48	25	16	10	1.11
Glu60Lys	1.0	17	17	3.6	51	16	30	6.4	0.33
Asp61Asn	0.39	21	53	28	59	17	32	15	0.72
Asp61Lys	0.82	15	19	8.5	58	14	37	7.2	0.19
Glu59Lys/Glu60Gln[b]	0.21	23	109	22	44	18	22	14	1.5

[a] The parameters were calculated from the data in Table 3 as described in the text.

The mechanistic parameters derived assuming the RE model are given in Table 5. k_{et}, k_{-et}, and k'_{off} were calculated from the observed parameters in the limit of high Pc concentrations given in Table 3 using the relations for the RE model in Table 2. The calculated k_{et} was then used together with the observed rate constant of the fast phase at low Pc concentration and the slopes k'_s and a'_f defined above to calculate k_{on}, k_{off}, and r ($=K_{diss}/K_{diss}^{red}$, where K_{diss} and K_{diss}^{red} are the dissociation constants before ET with P700 oxidized and reduced, respectively) (see the Theory section in Materials and Methods). The ET driving force within the complex (the difference in reduction potentials between P700 and Pc when Pc is bound to PS1) was calculated from $\Delta E_c^\circ = (RT/F)\ln(k_{et}/k_{-et})$. This is related to the difference ΔE_f° between the reduction potentials of free P700 [490 mV (*27*)] and Pc (Table 3) through the following thermodynamic relation:

$$\frac{RT}{F}\ln\frac{K'_{diss}}{K_{diss}} = \Delta E_f^\circ - \Delta E_c^\circ$$

where K_{diss} and K'_{diss} are the dissociation constants for the Pc−PS1 complex before and after the ET, respectively. The resulting K'_{diss} values are listed in Table 5.

Effect of Ionic Strength on the Kinetics. The effect of ionic strength on $P700^{ox}$ reduction was investigated at pH 7.5 by gradually adding $MgCl_2$ (from 0 to 90 mM). The studies were performed at a high Pc concentration (0.7 mM) with the purpose of trying to discriminate between the CC and RE models since they predict different kinetic behaviors when the binding site on PS1 is saturated with Pc (see the Discussion). A similar behavior is expected for the two models at low Pc concentrations. However, we had problems at low concentrations (around 50 μM) for several of the Pc mutants in that they seemed to be unable to transfer electrons to PS1 at an ionic strength above 100 mM.

For most of the Pc mutants at a concentration of 0.7 mM, there are only small variations in the rate constant of the fast phase, k_f, around the values determined at 7 mM $MgCl_2$ and reported in Table 3 (see Figure 6A). However, for wild type Pc (Figure 6A, ●) as well as for the mutants Glu60Lys (Figure 6A, □) and Asp61Asn (not shown), there is a significant increase in k_f with about 20% in the investigated ionic strength interval. For the Gln88Lys mutant, there is a slight drop in k_f at both low and high ionic strengths (Figure 6A, △).

The dispersion of the data points in Figure 6A is not uniform over the investigated range of ionic strength. The spread becomes larger at high ionic strengths (see Figure 6A, ●). This is because the fraction of the fast phase (a_f) is smaller at high ionic strengths (see Figure 6C), and this leads to a larger uncertainty in the fitted value of the corresponding rate constant (k_f). For a similar reason, the rate constant of the slow phase (k_s) exhibits a larger dispersion at low ionic strengths (Figure 6B) where its relative amplitude is small (a_f is large; see Figure 6C).

Overall, the rate constant of the slow phase, k_s, and the amplitude ratio, a_f, both decrease monotonically with increasing ionic strength for wild type Pc and the mutants that were studied (panels B and C of Figure 6, respectively). The Asp61Lys mutant is an exception in that k_s decreases when going to very low ionic strengths (Figure 6B, ◆). A striking feature displayed by the Glu60Lys (Figure 6, □) and Glu60Gln (not shown) mutants is the fact that the ionic strength dependence is very weak. Both k_s and a_f decrease very little with increasing ionic strength. A general feature of most mutants is also that the decrease in k_s is not uniform. After an initial decrease, a plateau is reached around 50 mM, and then k_s drops more rapidly as the ionic strength is increased (Figure 6B).

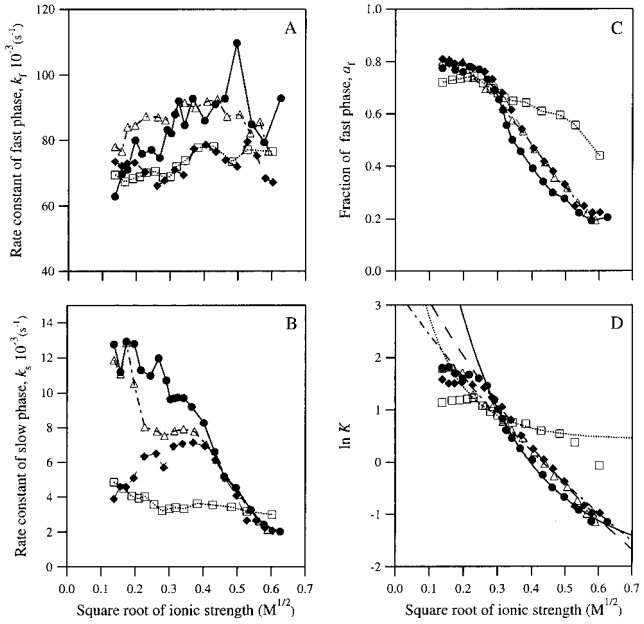

FIGURE 6: Effect of ionic strength on the reduction kinetics of photooxidized P700 by wild type plastocyanin (●) and the mutants Glu60Lys (□), Asp61Lys (◆), and Gln88Lys (△). The experimental conditions were as described in the legend of Figure 4 except that the plastocyanin concentration was 0.7 mM, the cuvette thickness was 2 mm, and the ionic strength was varied by addition of small aliquots of a concentrated $MgCl_2$ solution. The panels show the rate constants of the fast (k_f, A) and slow phases (k_s, B) and the fraction of the fast phase (a_f, C). Panel D shows the natural logarithm of the equilibrium constant K calculated from the data in panels A−C. K corresponds to K_{dc} and K_{et} in the CC and RE models, respectively. The curves were obtained by fitting the data to a parallel-plate model. See the text for details.

Using the observed parameters reported in Figure 6A−C, it is possible to calculate the equilibrium constants K_{dc} and K_{et} in the CC and RE models, respectively. The numerical values are the same, and the result has been plotted in Figure 6D as ln(K) versus ionic strength. With the exception of the mutants in position 60, all Pc proteins display a similar behavior: After an initial plateau at low ionic strengths, ln(K) decreases with a similar slope and eventually levels off at high ionic strengths. The slope is significantly lower for the Glu60Lys (Figure 6D, □) and Glu60Gln mutants (not shown).

DISCUSSION

An alignment of 24 plant, six algal, and seven cyanobacterial Pc sequences shows that residues 42−44 in the large acidic patch are identical in plants and algae. The small acidic patch exhibits a lower degree of conservation. Glu59 is replaced with a glutamine in four plant sequences. The residue in position 60 does not carry a negative charge in four plant sequences, and it is deleted in algae. The highest conserved residue in the small acidic patch is the aspartate (or glutamate) in position 61, where a negative charge is found in all eukaryotic sequences but one. In the cyanobacterial Pc sequences, residues 59−61 are often histidine, lysine, and glutamine, respectively, but the degree of conservation is lower.

Site-directed mutagenesis studies in this and earlier work have shown that the association between Pc and PS1 is governed by both electrostatic and hydrophobic interactions. Mutations in the large acidic patch have been shown to influence the ET reaction to a larger extent than mutations in the small acidic patch (*5*, *10*, *11*, *19*). However, mutations in the small acidic patch have larger effects on the reduction potential because of the shorter distance to the copper site, and this could have effects on the driving force for ET.

In this work, we have studied the effect of single mutations in the small acidic patch of Pc on the reactivity with PS1. Single mutations generally result in small structural changes within the closest vicinity, and they are expected to have only small effects on packing and thereby on protein stability. A distortion in the packing upon mutation is often accommodated by a small structural reorganization of the overall structure. To reduce any size effects of the mutations on the Pc structure as well as on the interaction with PS1, the aspartate in position 61 was replaced with an asparagine and the glutamates at positions 59 and 60 were replaced with glutamines. No changes in their spectral parameters were observed, nor was there any effect upon substituting these residues with a lysine. This is expected since these residues are surface-exposed and quite far from the copper site. The glutamine residue at position 88 is more buried and closer to the copper site (the neighboring His87 is a copper ligand). A lysine in this position might therefore influence both the stability of the protein and the geometry of the copper site. Since copper is known to stabilize the folded structure of type 1 copper proteins (*28*, *29*), a distorted geometry may result in a less stable protein, lower expression levels, and altered spectral characteristics. However, no change either in the reduction potential or in the spectral parameters was observed for this mutation. The wild type-like characteristics of the mutant proteins suggest a structure similar to that of the wild type and suggest that the same kinetic mechanism can be used in the evaluation of the kinetic data.

Effect of Pc Concentration on the Kinetics. The observed kinetic parameters presented in Table 3 show that the fast phase is largely unaffected by the mutations. The maximum value of the rate constant of the slow phase (k_{smax}) is reduced by about 50% by the Glu60Gln, Glu60Lys, and Asp61Lys mutations, and this implies that the equilibrium for the ET step (RE model) or the conformational change (CC model) has been affected. The half-saturating values of the slow phase (C_{ks}) and the fraction of fast phase (C_{af}) are reached already at low Pc concentrations. The opposite is observed for the Glu59Lys mutant, which exhibits higher half-saturating concentrations than the wild type. These effects reflect changes in the binding to PS1.

One purpose of the work presented here is to compare two theoretical models for the interaction between Pc and PS1, the CC and RE models. In the following, it will be shown that both models can be used to explain the Pc concentration dependence of the kinetics for the different Pc mutants.

The observed parameters can be interpreted assuming the CC model. The binding to PS1 is stronger for the Glu60Gln, Glu60Lys, and Asp61Lys mutants than for the wild type Pc as evidenced by their smaller dissociation constants given in Table 4. An effective dissociation constant that takes into account binding of Pc in both the inactive and active conformations can be calculated, and the conclusion is similar. The largest contribution to the lower effective dissociation constant comes from k_{on} since the k_{off} and K_{dc}

values of these mutants are similar to those of the wild type. It should be noted, however, that the individual values for k_{off} and k_{on} calculated in the CC model are less reliable than their ratio, i.e., K_{diss}. This was learned from simulations of the type described in Figure 3, which showed only small variations in the observable kinetics when k_{on} and k_{off} were changed by similar amounts. The Glu59Lys mutant reveals an increased dissociation constant, and its ET rate was the one most affected despite the wild type-like reduction potential.

The rearrangement between the inactive and active conformations was hindered in both directions in the Glu60Gln, Glu60Lys, and Asp61Lys mutants but to similar extents, resulting in a K_{dc} similar to the wild type value. The rearrangement to the active conformation was promoted by the Gln88Lys mutation, and an ET rate constant higher than that for the wild type Pc was observed. This residue has previously been replaced with a glutamate and an asparagine with preserved wild type-like kinetics (*6*, *30*). This residue is a glutamine in most eukaryotic Pc sequences; however, an alanine is sometimes found here. In the seven aligned cyanobacterial sequences, the residue in this position is always an arginine. A positive charge in this position may favor an active conformation in which the ET rate constant is higher.

The data can also be interpreted on the basis of the RE model. At low Pc concentrations, the behavior of both models reflects the binding process and thus similar conclusions are drawn. Note, however, that the dissociation constants calculated with the RE model (Table 5) are generally larger than the effective dissociation constant calculated with the CC model (Table 4). Three mutants, the same as in the CC model, exhibited an increased level of binding to reduced PS1 as indicated by their low dissociation constants (18% of the wild type value). The Glu59Lys mutant exhibited an increased dissociation constant. The equilibrium constant for the ET (related to the driving force in the complex, ΔE_c°) corresponds to K_{dc} in the CC model. In the RE model, this equilibrium is dependent on the dissociation constant after ET, K'_{diss}. The latter was most reduced in the Glu60Lys and Asp61Lys mutants, which have a stronger binding to PS1 even after the electron has been transferred. The faster kinetics observed for the Gln88Lys mutant are consistent with its higher driving force for ET within the complex.

One important consequence of using the RE model in the data interpretation is that the dissociation constant after ET seems to be much larger than before ET. This applies to all Pc mutants studied here as well as to wild type Pc. For the wild type protein, Pc^{ox} binds 38 times weaker than Pc^{red} to PS1 with P700 in the reduced state (cf. K'_{diss} and K^{red}_{diss} in Table 5). As a comparison, Drepper et al. found a 6 times larger dissociation constant for Pc^{ox} than for Pc^{red} (*18*). This change was suggested to be due to a diminished electrostatic attraction between Pc and PS1 since the net negative charge of Pc decreases by 1 upon oxidation. Another possibility is that the structure of the metal site and the protein surface around His87 changes upon oxidation as suggested in a recent study with perturbed angular correlation spectroscopy (*25*). The metal site structure was found to be slightly different in the Ag^+ and Cd^{2+} derivatives of Pc (which mimic the Cu^+ and Cu^{2+} forms, respectively), and a loss of complementarity between the two protein surfaces could explain why Cd−Pc binds at least 24 times weaker to PS1 than Ag−Pc. It should be noted that the CC model does not exclude the possibility that Pc^{ox} and Pc^{red} can bind with different strengths to PS1. However, inclusion of this possibility in the model leads to more mechanistic parameters than can be assigned from the observable parameters in our kinetic studies.

To conclude, both models can provide reasonable explanations for the observed kinetics, and it is not possible to discriminate between the models. However, in this work, we have emphasized the kinetic data obtained in the limits of low and high Pc concentrations. At intermediate concentrations (around 100 μM), we predict that the P700 reduction kinetics are triphasic (see the Theory section in Materials and Methods and Figure 3) and that the two models should behave differently. Preliminary analysis of data for wild type Pc acquired at an improved signal-to-noise ratio indeed indicates the presence of a third phase with a rate constant intermediate between the two reported here (K. Olesen and Ö. Hansson, unpublished results).

Irrespective of which model is used for the data interpretation, some general conclusions can be drawn about the effect of the mutations. Evidently, changing the negative charge at position 60 or 61 to a positive results in a stronger binding between Pc^{red} and PS1. One may therefore ask why these negative charges are conserved to such a high degree among eukaryotic sequences (see above). However, an excessively strong binding of Pc^{red} may not be an evolutionary advantage since then Pc^{ox} also may bind strongly which will limit the overall turnover of the ET chain. There is also a possibility that the negative charges are necessary for a favorable interaction with cyt *f*. The high degree of conservation of Gln88 may also indicate that this residue is important for the latter interaction despite our finding that a lysine in this position results in a faster ET to PS1.

Effect of Ionic Strength on the Kinetics. Both the RE and CC models can be used to interpret the influence of Pc concentration on the $P700^{ox}$ reduction kinetics, at least in the limits of low and high Pc concentrations. To discriminate between the two models, we decided to investigate how well they can account for the ionic strength dependence of the kinetics. Both models predict a similar behavior at low Pc concentrations since the kinetics are mainly determined by the binding of Pc to PS1. However, at high Pc concentrations, the presence of two kinetic phases is mainly due to the equilibrium between the C_2 and C_3 states (see the Theory section in Materials and Methods). In the CC model, this step corresponds to a conformational change in the Pc−PS1 complex, while in the RE model, it represents a reversible ET. As outlined below, these processes are expected to be affected differently by changes in ionic strength. The equilibrium constant for this process (K) has been calculated from the observed kinetic parameters and found to decrease as the ionic strength is increased (see Figure 6D). In this context, it is worth pointing out that the ionic strength dependence of equilibrium constants is generally more amenable to a theoretical analysis than that of individual mechanistic rate constants such as k_{on} and k_{off}. The theoretical expressions for these are much more complicated than those for equilibrium constants (*31*).

In the RE model, K corresponds to K_{et} which is thermodynamically related to the dissociation constants for the Pc−PS1 complex before (K_{diss}) and after (K'_{diss}) the ET:

$$\ln K_{et} = \frac{F\Delta E_f^\circ}{RT} + \ln\frac{K_{diss}}{K'_{diss}}$$

where ΔE_f° is the difference between the reduction potentials of free P700 and Pc. Since dissociation constants are proportional to exp(V/RT), where V is the electrostatic potential of the complex, we have

$$RT \ln\frac{K_{diss}}{K'_{diss}} = V - V'$$

where V' is the electrostatic potential after the ET. The particular choice of V is not critical for the arguments to follow, but assuming a simple parallel-plate model as a concrete example (*32*), we have

$$V(\kappa) = z_D z_A \alpha f(\kappa)$$

where $f(\kappa) = \exp(-\kappa\rho)/(1 + \kappa\rho)$ is a function decreasing with a κ of $(3.295\ \mathrm{nm}^{-1})\sqrt{I}$, ρ is the radius of the plates, α is a positive constant independent of κ, and z_D and z_A are the charges of the electron donor (Pc) and acceptor (PS1), respectively. If we assume that only the charges change during the ET (to $z'_D = z_D + 1$ and $z'_A = z_A - 1$) and if we neglect the small ionic-strength dependence in ΔE_f° (*33*), then

$$\ln K_{et} = c_\infty + c_0 f(\kappa)$$

where $c_\infty = F\Delta E_f^\circ/RT$ and $c_0 = z_D - z_A + 1$. Since we expect c_∞ to equal ≈4 and c_0 to be less than 0 for the Pc−PS1 complex, ln K_{et} should increase with ionic strength from $c_\infty + c_0$ to c_∞ if the RE model is effective.

The equilibrium constant that we have plotted in Figure 6D decreases with ionic strength. The data at high ionic strength can be well fitted to a parallel-plate model with a c_0 of 12 and a c_∞ of −2 for wild type Pc. This is inconsistent with the RE model which we therefore consider less likely. The data are, however, not in conflict with the CC model. In this case, the equilibrium constant corresponds to K_{dc}, which is expected to decrease with ionic strength since the electrostatic interactions favor the active conformation.

CONCLUSION

Changes in the small acidic patch of Pc result in significant effects on the ET to PS1, but the effects are not as strong as when residues in the large acidic patch are modified. The small acidic patch is important for fine-tuning the reaction, and it is critical for the ionic strength dependence. One residue in the small acidic patch, Glu60, seems to be responsible for the major part of the ionic strength dependence of the kinetics. At high Pc concentrations, this dependence is consistent with the CC model but not with the RE model. Future prospects would include systematic studies of the large acidic patch by site-directed mutagenesis and a thorough study of the ionic strength dependence of such mutants as well as kinetic studies with an improved signal-to-noise ratio at intermediate Pc concentrations.

ACKNOWLEDGMENT

Ö.H. is grateful for enlightening discussions with Eva Danielsen.

REFERENCES

1. Marcus, R. A., and Sutin, N. (1985) *Biochim. Biophys. Acta 811*, 265−322.
2. Bendall, D. S. (1996) in *Protein Electron Transfer*, BIOS Scientific Publishers Ltd., Oxford, U.K.
3. Xue, Y., Ökvist, M., Hansson, Ö., and Young, S. (1998) *Protein Sci. 7*, 2099−105.
4. Haehnel, W., Jansen, T., Gause, K., Klosgen, R. B., Stahl, B., Michl, D., Huvermann, B., Karas, M., and Herrmann, R. G. (1994) *EMBO J. 13*, 1028−38.
5. Hippler, M., Reichert, J., Sutter, M., Zak, E., Altschmied, L., Schroer, U., Herrmann, R. G., and Haehnel, W. (1996) *EMBO J. 15*, 6374−84.
6. Sigfridsson, K., Young, S., and Hansson, Ö. (1996) *Biochemistry 35*, 1249−57.
7. Wynn, R. M., and Malkin, R. (1988) *Biochemistry 27*, 5863−9.
8. Takabe, T., Ishikawa, H., Niwa, S., and Tanaka, Y. (1984) *J. Biochem. (Tokyo) 96*, 385−93.
9. Anderson, G. P., Sanderson, D. G., Lee, C. H., Durell, S., Anderson, L. B., and Gross, E. L. (1987) *Biochim. Biophys. Acta 894*, 386−98.
10. Lee, B. H., Hibino, T., Takabe, T., and Weisbeek, P. J. (1995) *J. Biochem. (Tokyo) 117*, 1209−17.
11. Young, S., Sigfridsson, K., Olesen, K., and Hansson, Ö. (1997) *Biochim. Biophys. Acta 1322*, 106−14.
12. Qin, L., and Kostić, N. M. (1993) *Biochemistry 32*, 6073−80.
13. Ullmann, G. M., Knapp, E.-W., and Kostić, N. M. (1997) *J. Am. Chem. Soc. 119*, 49−52.
14. Ubbink, M., Ejdebäck, M., Karlsson, B. G., and Bendall, D. S. (1998) *Structure 6*, 323−35.
15. Hervas, M., Navarro, J. A., Diaz, A., Bottin, H., and De la Rosa, M. A. (1995) *Biochemistry 34*, 11321−6.
16. Bottin, H., and Mathis, P. (1985) *Biochemistry 24*, 6453−60.
17. Sigfridsson, K., Hansson, Ö., Karlsson, B. G., Baltzer, L., Nordling, M., and Lundberg, L. G. (1995) *Biochim. Biophys. Acta 1228*, 28−36.
18. Drepper, F., Hippler, M., Nitschke, W., and Haehnel, W. (1996) *Biochemistry 35*, 1282−95.
19. Hibino, T., Lee, B. H., Yajima, T., Odani, A., Yamauchi, O., and Takabe, T. (1996) *J. Biochem. (Tokyo) 120*, 556−63.
20. Ejdebäck, M., Young, S., Samuelsson, A., and Karlsson, B. G. (1997) *Protein Expression Purif. 11*, 17−25.
21. Landt, O., Grunert, H. P., and Hahn, U. (1990) *Gene 96*, 125−8.
22. Boardman, N. K. (1971) *Methods Enzymol. 23*, 268−76.
23. Dutton, P. L., and Prince, R. C. (1978) in *The Photosynthetic Bacteria* (Clayton, R. K., and Sistrom, W. R., Eds.) pp 525−70, Plenum Press, New York.
24. Drepper, F., Dorlet, P., and Mathis, P. (1997) *Biochemistry 36*, 1418−27.
25. Danielsen, E., Scheller, H. V., Bauer, R., Hemmingsen, L., Bjerrum, M. J., and Hansson, Ö. (1999) *Biochemistry 38*, 11531−40.
26. Ejdebäck, M. (1999) Ph.D. Thesis, Göteborg University, Göteborg, Sweden.
27. Nordling, M., Sigfridsson, K., Young, S., Lundberg, L. G., and Hansson, Ö. (1991) *FEBS Lett. 291*, 327−30.
28. Merchant, S., and Bogorad, L. (1986) *J. Biol. Chem. 261*, 15850−3.
29. Leckner, J., Bonander, N., Wittung-Stafshede, P., Malmström, B. G., and Karlsson, B. G. (1997) *Biochim. Biophys. Acta 1342*, 19−27.

30. Sigfridsson, K., Young, S., and Hansson, Ö. (1997) *Eur. J. Biochem. 245*, 805−12.
31. van Leeuwen, J. W. (1983) *Biochim. Biophys. Acta 743*, 408−21.
32. Watkins, J. A., Cusanovich, M. A., Meyer, T. E., and Tollin, G. (1994) *Protein Sci. 3*, 2104−14.
33. Niles McLeod, D. D., Freeman, H. C., Harvey, I., Lay, P. A., and Bond, A. M. (1996) *Inorg. Chem. 35*, 7156−65.
34. Koradi, R., Billeter, M., and Wüthrich, K. (1996) *J. Mol. Graphics 14*, 51−5.

BI991242I